

TOWARD UNRAVELLING THE STRUCTURAL DISTRIBUTION OF ULTRA-HIGH-ENERGY COSMIC RAY SOURCES

HAJIME TAKAMI¹ AND KATSUHIKO SATO^{1,2,3}

Received 2007 October 3; accepted 2008 January 25

ABSTRACT

We investigate the possibility that observations of ultra-high-energy cosmic rays (UHECRs) in the near future may be able to unveil their local source distribution, which will reflect observed local structures if their origins are astrophysical objects. In order to discuss this possibility, we calculate the arrival distribution of UHE protons taking into account their propagation process in intergalactic space, i.e., energy losses and deflections by the extragalactic magnetic field (EGMF). For a realistic simulation, we construct and adopt a model of a structured EGMF and UHECR source distribution, which reproduces the local structures actually observed around the Milky Way. The arrival distribution is compared statistically to the source distribution using a correlation coefficient. We find that UHECRs above $10^{19.8}$ eV are the best indicators for deciphering the source distribution within 100 Mpc, and the detection of about 500 events on all the sky would allow us to unveil the local structure of the UHE universe for plausible EGMF strength and source number density. This number of events could be detected by 5 years observation by the Pierre Auger Observatory.

Subject headings: cosmic rays — galaxies: general — ISM: magnetic fields — large-scale structure of universe — methods: numerical

1. INTRODUCTION

The origin of ultra-high-energy cosmic rays (UHECRs) above 10^{19} eV is one of the most intriguing problems in astroparticle physics. The Akeno Giant Air Shower Array (AGASA) found statistically significant small-scale clusterings of observed UHECR events with large-scale isotropy (Takeda et al. 1999). The AGASA data set of 57 events above 4×10^{19} eV contains four doublets and one triplet within a separation angle of 2.5° , consistent with the experimental angular resolution. The chance probability of observing such multiplets under an isotropic distribution is only about 1% (Hayashida et al. 2000). A combination of the results of many UHECR experiments (including AGASA) also revealed eight doublets and two triplets within 4° among 92 events above 4×10^{19} eV (Uchihori et al. 2000). These multiplets suggest that the origins of UHECRs are pointlike sources. For identification of UHECR sources, arrival directions of UHECRs have been observed in detail by the High Resolution Fly’s Eye (HiRes) and Pierre Auger Observatory (Auger). However, so far these experiments have reported no significant clustering in the arrival distribution above 4×10^{19} eV (Abbasi et al. 2005a; Mollerach et al. 2007).

Recently, several classes of astrophysical objects have been tested for positional correlations with observed arrival directions of UHECRs. The correlations with BL Lac objects were discussed on the assumption of smaller deflection angles of UHECRs than the experimental angular resolution and/or neutral primaries (Tinyakov & Tkachev 2001), and considering deflection by the Galactic magnetic field (GMF) (Tinyakov & Tkachev 2002). Gorbunov & Troitsky (2005) considered various classes of powerful extragalactic sources for their correlation study, including small corrections of UHECR arrival directions by GMF. Hague

et al. (2007) discussed the correlation with nearby active galactic nuclei (AGNs) from the *RXTE* catalog of AGNs. However, these studies have not taken into account UHECR propagation in extragalactic space. UHECRs above 8×10^{19} eV lose a significant fraction of their energy by photopion production in collision with cosmic microwave background (CMB) photons during their propagation (Berezinsky & Grigorieva 1988; Yoshida & Teshima 1993). Thus, UHECRs have *horizons*, which are the maximum distances of their sources from which UHECRs can reach the Earth, even if their energies are below 8×10^{19} eV at the Earth. The positional correlations between arrival directions of UHECRs and their source candidates outside the horizons are not significant. (In Hague et al. [2007], only nearby AGNs within the horizons are considered.) In addition to the UHECR horizons, deflections due to the extragalactic magnetic field (EGMF) are also important, since extragalactic cosmic rays are propagated for a much greater distance than in Galactic space. Propagation process of UHECRs should be considered in such correlation studies.

Yoshiguchi et al. (2003a) investigated the correlation between the arrival distribution of UHECRs and their source distribution, taking into account UHECR propagation in intergalactic space, with a uniform turbulent EGMF of strength 1 nG and coherent length 1 Mpc. The authors adopted a source distribution with 10^{-6} Mpc⁻³ that reproduced the local structures and the AGASA results. They concluded that detection of a few thousand events above 4×10^{19} eV reveal an observable correlation with sources within 100 Mpc.

However, a uniform turbulent field is not a realistic EGMF model. Faraday rotation measurements indicate magnetic field strengths at the μ G level within the inner regions (\sim central Mpc) of galaxy clusters (Kronberg 1994). The evidence for synchrotron emission in numerous galaxy clusters (Giovannini & Feretti 2000) and in a few cases of filaments (Kim et al. 1989; Bagchi et al. 2002) also seems to suggest the presence of magnetic fields of 0.1–1.0 μ G in cosmological structures.

Based on these studies, in recent years, we calculated the propagation of UHE protons in a structured EGMF which well reproduces the local structures actually observed, and simulated

¹ Department of Physics, School of Science, University of Tokyo, 7-3-1 Hongo, Bunkyo-ku, Tokyo 113-0033, Japan.

² Research Center for the Early Universe, School of Science, University of Tokyo, 7-3-1 Hongo, Bunkyo-ku, Tokyo 113-0033, Japan.

³ Institute of Physics and Mathematics for the Universe, University of Tokyo, Kashiwa, Chiba, 277-8582, Japan.

their arrival distributions with several normalizations of EGMF strength and several number densities of UHECR sources (Takami & Sato 2008). We constrained the source number density to best reproduce the AGASA results. As a result, 10^{-5} Mpc^{-3} is the most appropriate number density, which is weakly dependent on EGMF strength. (In rectilinear propagation, a similar number density is also obtained in Blasi & de Marco 2004; Kachelriess & Semikoz 2005.) However, this has large uncertainty due to the small number of observed events at present; 10^{-4} Mpc^{-3} and 10^{-6} Mpc^{-3} are also statistically possible. Therefore, it is useful to consider the correlation between the arrival distribution and the source distribution in the case of these number densities. Note that this uncertainty should be resolved by the future increase in detected events.

In this study, we calculate the arrival distribution of UHECRs, taking their propagation process into account, and investigate the potential correlation of the arrival distribution and their source distribution. A structured EGMF model and source distribution that can reproduce the local universe actually observed are adopted. The source number density and the EGMF strength are treated as parameters, since these have some uncertainty. One goal of this study is to understand the number of observed events, and to start to observe the UHECR source distribution with UHECRs, to gauge how much correlation we might expect to see in future observations.

Auger has already detected more events above 10^{19} eV than those observed by AGASA (Roth et al. 2007). Nevertheless, event clustering has not been observed, as mentioned above. This might be because the EGMF and/or GMF is strong enough to suppress the multiplets or statistical fluctuation for the small number of observed events at the highest energies. In any case, we should consider how the arrival distribution reflects the UHECR source distribution.

The chemical composition of UHECRs is very important for the correlation. If UHECRs have heavier components, magnetic deflections are larger and the correlation is worse. One of the observables for the study of UHECR composition is the depth of the shower maximum, X_{max} , which can be measured by fluorescence detectors. Its average value $\langle X_{\text{max}} \rangle$ is dependent on UHECR composition and energy. HiRes reported, as a result of X_{max} measurement, that the composition of cosmic rays above 10^{19} eV is dominated by protons (Abbasi et al. 2005b). Recent results by Auger are compatible with the HiRes results within systematic uncertainties (Unger et al. 2007). Another observable is the muon density from extensive air showers of UHECRs, as observed by ground arrays. Recent studies of the muon content indicate some fraction of heavier components in the highest energy cosmic rays (Engel et al. 2007; Glushkov et al. 2007). However, the interpretation of these two observables is dependent on hadronic interaction models, which include uncertainties at the UHE energy region. Thus, UHECR composition at the highest energies is controversial at present. Despite this, here we assume that all UHECRs are protons, since light composition is expected if a positional correlation between the arrival directions of UHECRs and their source candidates, which is main theme of this paper, is observed in the near future.

This paper is organized as follows. In § 2 we provide our models of UHECR source distribution and a structured EGMF. In § 3 we explain our calculation method for the arrival distribution with UHECR propagation and our statistical method. In § 4, we present the results of the correlation between the arrival distribution of UHE protons and their source distribution. We summarize this study in § 5.

2. SOURCE DISTRIBUTION AND MAGNETIC FIELD

In this section, our models of UHECR source distribution and a structured EGMF are briefly explained. These models are almost the same as those in our previous work. More detailed explanations are given in Takami et al. (2006).

These models are constructed from the *Infrared Astronomical Satellite* Point Source Catalogue Redshift Survey (*IRAS* PSCz) catalog of galaxies (Saunders et al. 2000). This is a flux-limited galaxy survey with large sky coverage ($\sim 84\%$ of all the sky), and thus is an appropriate catalog for our purpose. The selection effects for observations are corrected with the luminosity function of the *IRAS* catalog (Takeuchi et al. 2003). We use a set of galaxies within 100 Mpc after correction (referred to as simply our sample galaxies below) to construct our models, since a small number of galaxies can be observed above 100 Mpc. We adopt $\Omega_m = 0.3$, $\Omega_\Lambda = 0.7$, and $H_0 = 71 \text{ km s}^{-1} \text{ Mpc}^{-1}$ as the cosmological parameters.

We assume that subsets of our sample galaxies with specific number densities of 10^{-4} , 10^{-5} , and 10^{-6} Mpc^{-3} are UHECR source distributions. For the source number densities, we randomly select galaxies from our sample galaxies with probabilities proportional to the absolute luminosity of each galaxy. This method allows us to construct source distributions to reflect the cosmic structures. It is assumed that the source distribution above 100 Mpc is isotropic, and that the luminosity distribution of galaxies follows the luminosity function. We take sources up to 1 Gpc into account. All sources are assumed to have the same power for injection of UHE protons.

Our EGMF model also reproduces the local structures actually observed around the Milky Way. Several simulations of cosmological structure formation with magnetic field have found that the EGMF roughly traces baryon density distribution. (Sigl et al. 2003; Dolag et al. 2005). Our structured EGMF model is constructed with simple assumptions in addition to these results. We constructed a matter density distribution from our sample galaxies with a spatial resolution of 1 Mpc equal to the correlation length of our EGMF model, l_c . In each cell, the strength of the EGMF is related to the matter density, ρ , as $|B_{\text{EGMF}}| \propto \rho^{2/3}$, and a turbulent magnetic field with the Kolmogorov spectrum is assumed. The strength of the EGMF is normalized to $B = 0.0, 0.1, \text{ and } 0.4 \mu\text{G}$ at a cell that contains the center of the Virgo Cluster, since EGMF strength has some uncertainty, as mentioned in § 1. These three normalizations are used to investigate the spatial correlation between the arrival distribution and the source distribution. Since the EGMF model and the source distribution are constructed from the same galaxy sample, UHECR sources are within the magnetized structure. Note that about 95% of the volume has no magnetic field in our EGMF model.

3. METHOD OF CALCULATION

3.1. Calculation of Arrival Distribution of UHE Protons

Once a source distribution is given, the arrival distribution of UHE protons can be calculated by calculating the propagation of protons from their sources to the Earth. In this section, we describe fundamental processes for proton propagation in intergalactic space and our method for calculating the arrival distribution.

UHE protons lose their energies in collision with CMB during their propagation in intergalactic space (Berezinsky & Grigorjeva 1988; Yoshida & Teshima 1993). Higher energy photon backgrounds (e.g., infrared, optical, ultraviolet) are neglected in this study, since we treat only protons above $10^{19.6} \text{ eV}$. Such protons remain nearly unaffected by the higher energy background

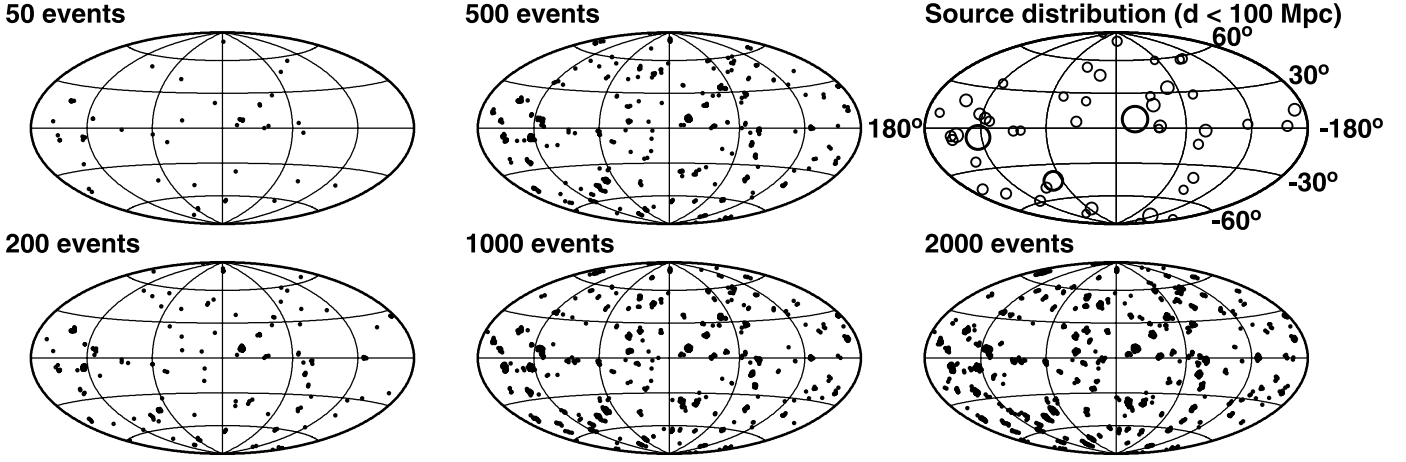


FIG. 1.— Arrival distributions of UHE protons above $10^{19.8}$ eV predicted by a specific source distribution with 10^{-5} Mpc^{-3} (upper right) in Galactic coordinates. The EGMF is not included. The source distribution within 100 Mpc is shown as radii of circles inversely proportional to source distances. The sources within 50 Mpc are shown with bold circles. Panels show 50 (upper left), 200 (lower left), 500 (upper middle), 1000 (lower middle), and 2000 (lower right) simulated events.

photons because of their relatively small number. Protons above 8×10^{19} eV lose energy by photopion production, $p + \gamma \rightarrow \pi + X$. This reaction has a large inelasticity ($\sim 30\%$) and a relatively short energy-loss length of a few tens of Mpc at $z = 0$. Protons with such energies cannot reach the Earth from distant sources. Thus, photopion production predicts a sharp spectral steepening around 8×10^{19} eV, the Greisen-Zatsepin-Kuz'min (GZK) steepening (Greisen 1966; Zatsepin & Kuz'min 1966). The GZK effect is essential in considering the correlation with distribution for relatively distant sources. We adopt the energy-loss length that is calculated by simulating the photopion production with the event generator SOPHIA (Mucke et al. 2000). On the other hand, protons below 8×10^{19} eV lose energy mainly due to Bethe-Heitler pair creation, $p + \gamma \rightarrow p + e^+ + e^-$. This has a small inelasticity ($\sim 10^{-3}$). We adopt the analytical fit function given by Chodorowski et al. (1992) to calculate the energy-loss rate for isotropic photons. Adiabatic energy loss due to the expanding universe also makes protons lose energy. The energy-loss rate can be written as

$$\frac{dE}{dt} = -\frac{\dot{a}}{a}E = -H_0[\Omega_m(1+z)^3 + \Omega_\Lambda]^{1/2}E. \quad (1)$$

These three energy-loss processes are treated as continuous processes in our calculation.

The trajectories of protons are deflected by the EGMF. Protons ejected from their sources toward the Earth cannot all reach Earth straightforwardly. It wastes much CPU time to calculate the propagation of protons that cannot reach Earth in order to construct the arrival distribution. To solve this problem, we suggest a new method for calculating the arrival distribution, an application of the back-tracking propagation (Takami et al. 2006). In this method, protons with a charge of -1 are ejected from the Earth, and we calculate their trajectories in intergalactic space, taking into account magnetic deflections and energy loss (or gain) processes. Such trajectories are then regarded as those of protons from extragalactic space. We calculate only trajectories of protons that can reach the Earth.

In order to simulate the arrival distribution, 2,500,000 protons (with charges of -1) with $dN/d \log_{10}E \propto \text{const}$ from 10^{19} to 10^{21} eV are ejected isotropically from the Earth. We calculate their trajectories until their propagation time exceeds the lifetime of the universe or their energies reach 10^{22} eV, which corresponds to the

maximum acceleration energy at UHECR sources. For each source distribution, we calculate a factor for the trajectory of the j th particle, which represents the relative probability that the j th proton will reach the Earth,

$$P_{\text{selec}}(E, j) \propto \sum_i \frac{1}{(1+z_{i,j})d_{i,j}^2} \frac{dN/dE_g(d_{i,j}, E_g^i)}{E^{-1.0}} \frac{dE_g}{dE}. \quad (2)$$

Here i labels sources on each trajectory, $z_{i,j}$ and $d_{i,j}$ are their redshift and distance, respectively, and E_g^i is the energy of a proton at the i th source, which has energy E at the Earth. Thus, $dN/dE_g(d_{i,j}, E_g^i) \propto E_g^{-2.6}$ is the energy spectrum of UHE protons ejected from a source whose distance is $d_{i,j}$. This spectral index, -2.6 , can reproduce the observed spectra from 10^{19} to 10^{20} eV well (De Marco et al. 2003), and corresponds to the proton-dip scenario (Aloisio et al. 2007). The term dE_g/dE is a correction factor for the variation of the shape of the energy spectrum through the propagation.

We randomly select trajectories according to these relative probabilities, P_{selec} , so that the number of selected trajectories is equal to the required event number. The mapping of the ejected direction of each particle from Earth can be regarded as the arrival distribution of UHE protons. If we have to select the same trajectory more than once to adjust the number of selected trajectories, we generate new events whose arrival direction is calculated by adding a normally distributed deviation with zero mean and variance equal to the experimental resolution to the original arrival direction. The experimental resolution is assumed to be 1° .

3.2. Statistical Quantities

In order to investigate statistically the similarity between the arrival distribution of UHECRs f_e and the source distribution f_s , a correlation coefficient between the two distributions is defined as

$$\Xi(f_e, f_s) \equiv \frac{\rho(f_e, f_s)}{\sqrt{\rho(f_e, f_e)\rho(f_s, f_s)}}, \quad (3)$$

where

$$\rho(f_a, f_b) \equiv \sum_{j,k} \frac{f_a(j, k) - \bar{f}_a}{\bar{f}_a} \frac{f_b(j, k) - \bar{f}_b}{\bar{f}_b} \frac{\Delta \Omega(j, k)}{4\pi}. \quad (4)$$

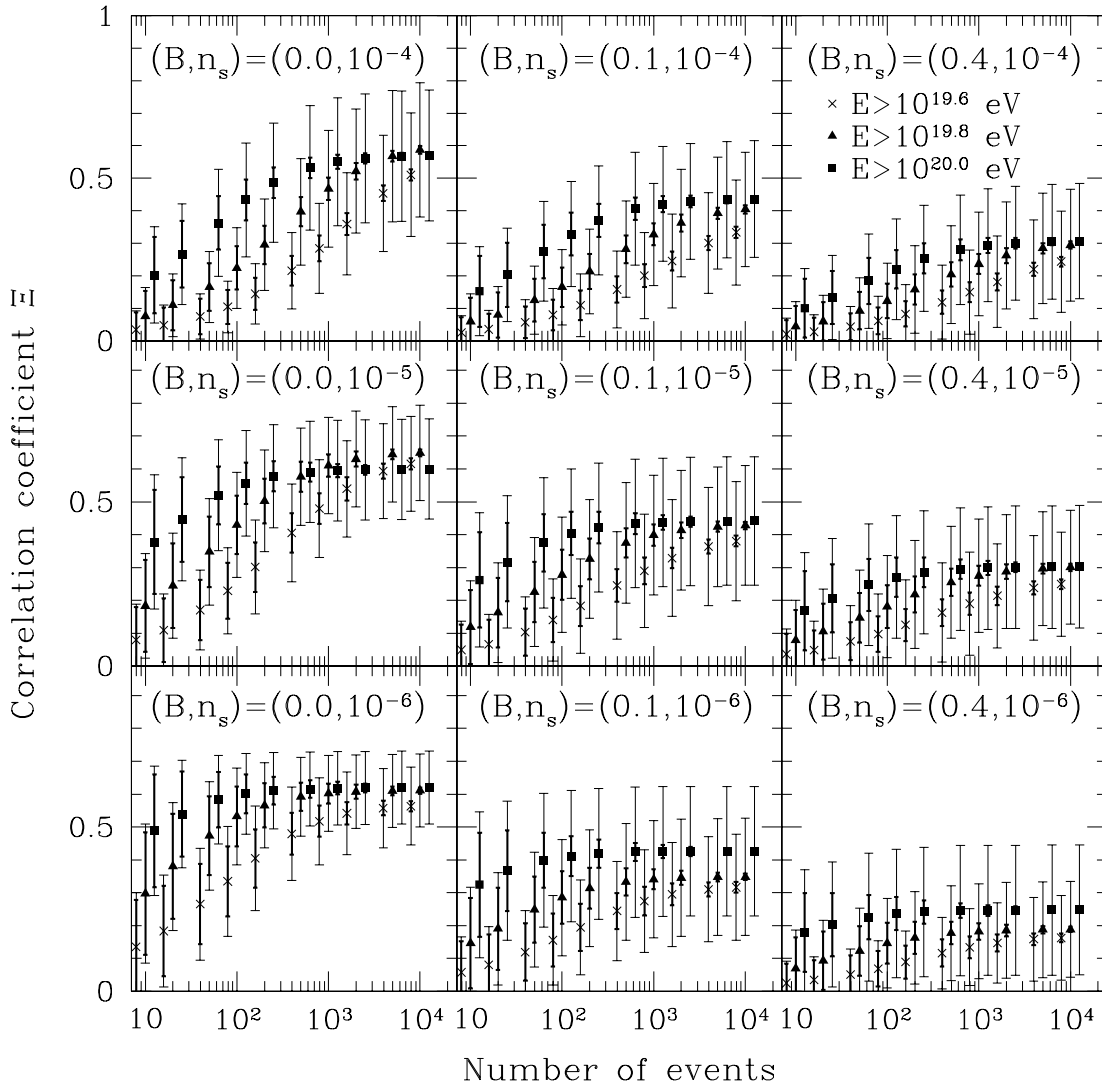


FIG. 2.— Correlation coefficients between the arrival distribution of UHE protons above $10^{19.6}$ (*crosses*), $10^{19.8}$ (*triangles*), and $10^{20.0}$ eV (*squares*), and their source distribution within 100 Mpc for several EGMF strengths and the number densities of UHECR sources as a function of expected number of cosmic rays on all the sky. The size of the cell for the calculation of the correlation coefficients is chosen to be $2^\circ \times 2^\circ$. The three marks for the same number of events are a little shifted horizontally for visibility. Units of B , normalization factor of the EGMF strength, and n_s , the source number density, are μG and Mpc^{-3} , respectively. The short (thick) error bars represent the fluctuations due to the finite number of observed events, and the long (thin) error bars are total errors including the cosmic variance.

Here the subscripts j and k distinguish each cell of the sky, $\Delta\Omega(j, k)$ denotes the solid angle of the (j, k) cell, and \bar{f}_a means the average of f , calculated as

$$\bar{f}_a \equiv \sum_{j,k} f_a(j, k) \frac{\Delta\Omega(j, k)}{4\pi}. \quad (5)$$

By definition, Ξ ranges from -1 to $+1$. When $\Xi = +1$ (-1), the two distributions are exactly the same (opposite). When $\Xi = 0$, we cannot find any resemblance between the two distributions. A source at a distance d_i approximately contributes to arriving cosmic rays with the weight of d_i^{-2} , since all sources are assumed to have the same injection power. Therefore, $f_s(j, k)$ is calculated as $\sum_i 1/d_i^2$, where i runs over sources in the (j, k) cell.

4. RESULTS

For a given source distribution, we can simulate the arrival distribution of UHE protons using the calculation method explained in § 3. We investigate the correlation between the arrival distribution and the source distribution, and discuss the possibility of unveiling the local structure through UHECRs.

In Figure 1, we show arrival distributions of UHE protons above $10^{19.8}$ eV predicted by a specific source distribution with 10^{-5}Mpc^{-3} in Galactic coordinates. The EGMF is not included. The source distribution within 100 Mpc is shown in the upper right panel. The radii of circles in this figure are inversely proportional to source distances. The sources within 50 Mpc are shown with bold circles. The number of simulated events are 50 (*upper left*), 200 (*lower left*), 500 (*upper middle*), 1000 (*lower middle*), and 2000 (*lower right*). Note that 50 events on all the sky corresponds to the current Auger results, since Auger observes cosmic rays in the southern hemisphere (Roth et al. 2007).

When 200 events are detected, strong event clusterings from nearby sources (within 50 Mpc) can be observed. The distribution of more distant sources has not yet been found, except in the directions where sources are positionally concentrated. Detection of more than 500 events would enable us to find event clusterings in the direction of almost all sources within 100 Mpc. Thus, we can find graphically that detection of about 500 cosmic rays above $10^{19.8}$ eV would enable us to unveil the nearby source distribution.

We should also discuss statistically (rather than graphically) the probability that future observations will be able to discern the UHECR source distribution. Figure 2 shows the predicted correlation coefficients between the arrival distribution of UHE protons and their source distribution within 100 Mpc for several EGMF strengths and source number densities as a function of expected number of cosmic ray events. The size of the cell for the calculation of the correlation coefficients is chosen to be $2^\circ \times 2^\circ$, since the angular resolution of UHECR experiments, 1° , is taken into account in simulating the arrival directions. The numbers of events for which we calculate the correlation coefficients are 10, 20, 50, 100, 200, 500, 1000, 2000, 5000, 10000 on all the sky for $E > 10^{19.6}$ (*crosses*), $E > 10^{19.8}$ (*triangles*), and $E > 10^{20.0}$ eV (*squares*). The three marks for the same number of events are slightly shifted horizontally for visibility. The EGMF strengths, B , and the source number densities, n_s , which are adopted for the simulation are represented on each panel. There are two errors. The thick (short) error bars show the statistical error, i.e., the fluctuations due to the finite number of observed events, averaged over 100 realizations of the source distribution for a given source number density. The random event selection used to estimate the fluctuations is performed 100 times for each source distribution. The thin (long) error bars represent the total error, i.e., the statistical error plus error due to different realizations of source distributions with the same number density. The latter error originates from our ignorance of a real source distribution. Since a real source distribution will be singular, the correlation coefficient in a real situation (observation) will converge on some value with only statistical error as the number of detected events increases.

First, we deliberate the correlation in the case of no magnetic field. Many features of the correlation coefficients common to finite EGMF cases are found in this simplest case. The three left panels of Figure 2 show the correlation coefficients in the case of no EGMF. When the number of observed events increases, the correlation coefficients start to converge, and the final value can be estimated. Errors from different source distributions remain for a large number of events. Thus, values of \mathcal{E} cannot be predicted with sufficient accuracy. (However, \mathcal{E} can be predicted for every source distribution with sufficient accuracy when the statistical errors are decreased due to an increased number of events.) Thus, we mainly discuss features common to each source distribution below. Note that the source distribution used in Figure 1 predicts correlation coefficients similar to the averages of those in the middle left panel of Figure 2.

The correlation coefficients cannot converge on 1.0 in spite of rectilinear propagation due to the finite angular resolution and the energy-loss processes, and also because cosmic rays do not always come from sources within 100 Mpc. Since UHE protons from more distant sources need a higher energy at the source in order to reach Earth with the same energy, such sources contribute fewer arriving cosmic rays than nearer sources even if a factor of d_i^{-2} is taken into account. In other words, the arrival distribution of many cosmic rays is only approximately the same spatial pattern as their source distribution weighted by d_i^{-2} .

We focus on the behaviors of the averages of the correlation coefficients in each panel. The correlation coefficients calculated for each source distribution behave with the same tendency. A source distribution that gives a smaller than average value for the correlation coefficient for a small number of events also predicts a smaller value for an increased number of events, and vice versa. Thus, the discussion below is applicable to each source distribution. Note that statistical errors for an observation are estimated as the thick error bars, since only one source distribution is realized in the universe.

The correlation coefficients with protons above 10^{20} eV predict larger values than those with lower energies for a small number of observed events. As the number of detected events increases, the coefficients for the highest energies converge on values a little smaller than those for lower energies. The reason for this is the GZK mechanism. UHE protons above 10^{20} eV can only come from sources within the GZK sphere (~ 50 Mpc). On the other hand, protons with lower energies can arrive at the Earth from outside 100 Mpc. Thus, the correlations are better for the smaller number of events. The difference between the correlation coefficients for protons above 4×10^{19} eV and those above 10^{20} eV is statistically significant at the 1σ level, as can be seen by the strengths of the observational errors, estimated as the thick error bars. Since the radius of the GZK sphere is less than 100 Mpc, there are sources within 100 Mpc that cannot be traced by cosmic rays above 10^{20} eV. Thus, as the number of observed events increases, the correlation coefficients for these highest energy protons converge on values a little smaller than those for lower energy protons. The correlations of protons with $E > 10^{19.8}$ eV are better than those with $E > 10^{19.6}$ eV, because lower energy protons can reach the Earth from more distant sources.

Next, we investigate the correlation including the EGMF. The middle and right panels of Figure 2 show the correlation coefficients for the case of $B = 0.1$ and $0.4 \mu\text{G}$, respectively. The EGMF diffuses trajectories of UHECRs during their propagation and obscures their arrival directions (Takami et al. 2006). Therefore, a stronger EGMF predicts a weaker correlation for any source number density. Compared to the correlation coefficient for the case of no EGMF, that of protons with a lower energy threshold is worse, since lower energy protons are more deflected by the EGMF. Protons with $E > 10^{19.6}$ and $10^{19.8}$ eV predict a smaller correlation than those above 10^{20} eV.

The number of events for which the correlation coefficients start to converge is weakly dependent on the EGMF strength and depends on the source number density. For 10^{-6} Mpc^{-3} , the required number of events is about 1000, 200, and 50 for $E > 10^{19.6}$, $10^{19.8}$, and 10^{20} eV respectively. At larger number densities, the number required for convergence increases. For 10^{-5} (10^{-4}) Mpc^{-3} , these numbers are about 5000 ($> 10,000$), 500 (5000), and 100 (500) for $E > 10^{19.6}$, $10^{19.8}$, and 10^{20} eV, respectively. Detection of this number of events should enable us to discern the UHECR source distribution at a visible level through UHE protons, which will be determined by the final value of the correlation coefficients. Both cosmic rays above $10^{19.8}$ eV and those above 10^{20} eV are good indicators for unravelling the source distribution, since their correlation values converge to nearly equal values for 10^{-4} and 10^{-5} Mpc^{-3} . However, the number of detected cosmic rays above $10^{19.8}$ eV reaches the number at which the correlation coefficients start to converge in a shorter observing period than cosmic rays above 10^{20} eV, since cosmic rays above 10^{20} eV are almost not detected in the presence of the GZK steepening. Note that our source model predicts the GZK steepening. Thus, UHE protons above $10^{19.8}$ eV are the best indicators for unveiling the source distribution within 100 Mpc. Note that ground-based detectors such as Auger and the Telescope Array (TA; Fukushima et al. 2007) can observe only about half of the hemisphere, so only half the arriving number will be observed.

Figure 3 shows a simulation of the arrival distribution of UHE protons above $10^{19.8}$ eV for the cases of $B = 0.1$ and $0.4 \mu\text{G}$. The source distribution is the same as in Figure 1. In Figures 1 and 3, the arrival distributions with 200 protons (less than 500 events, which is the number at which the correlation coefficients start to converge) includes several event clusterings. From a comparison

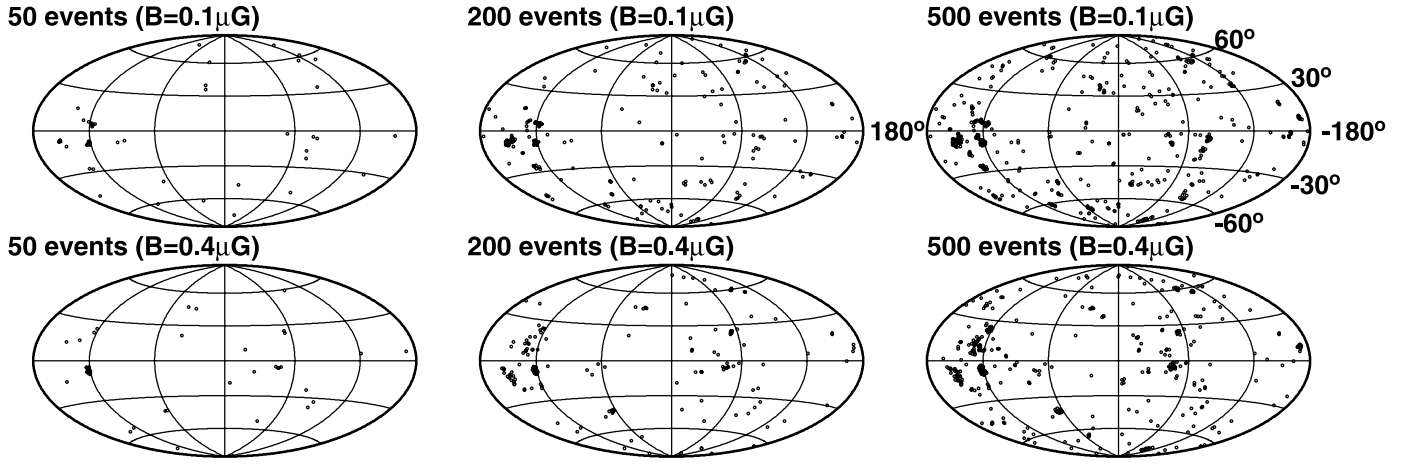


FIG. 3.— Arrival distributions of UHE protons above $10^{19.8}$ eV predicted by the same source distribution used in Fig. 2. The upper panels show those taking into account propagation in the EGMF with $B = 0.1 \mu\text{G}$; lower panels are the same, but for $B = 0.4 \mu\text{G}$.

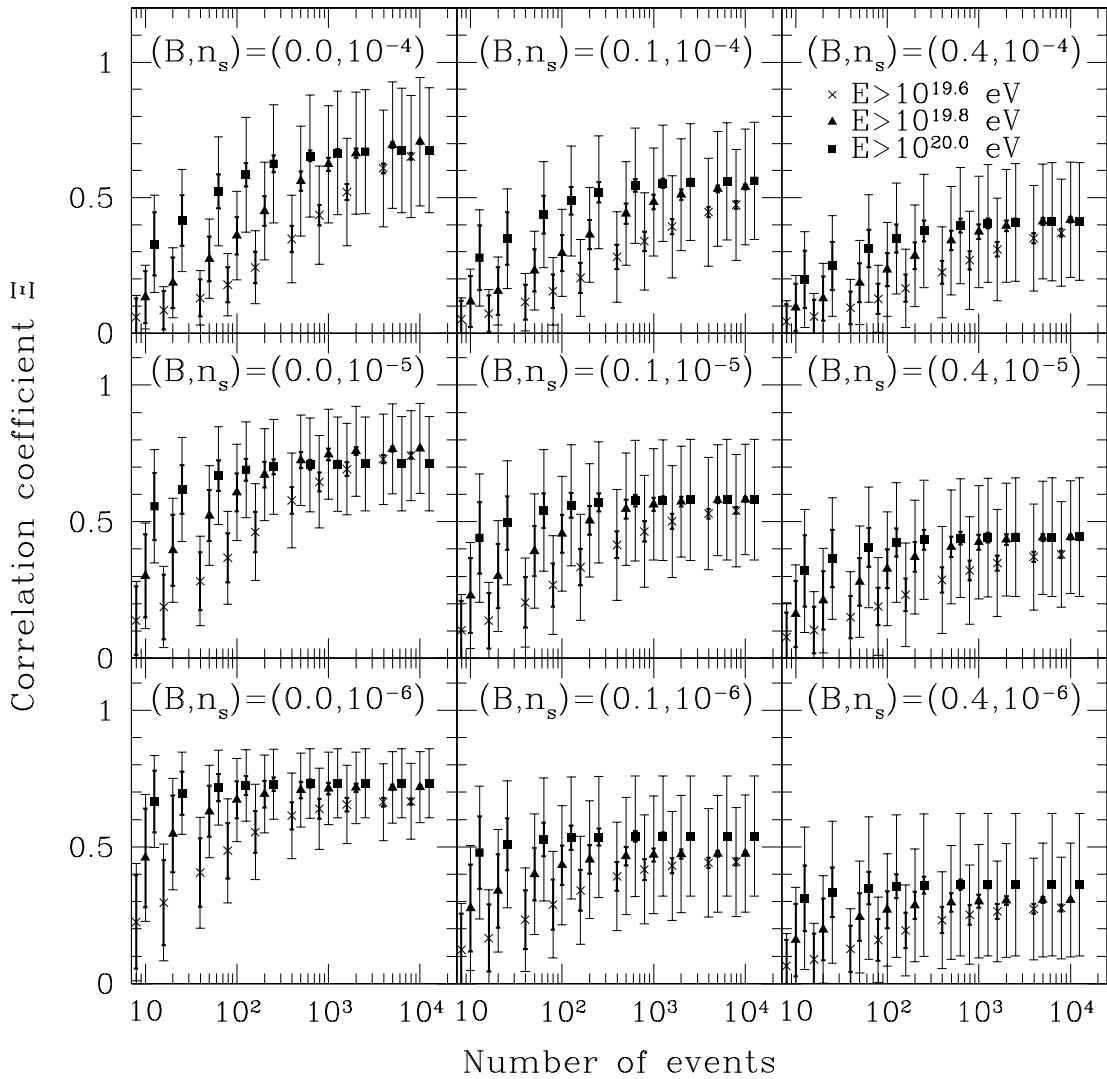


FIG. 4.— Same as Fig. 2, but for $4^\circ \times 4^\circ$.

to the three cases of different EGMF strength, we can see that the arrival directions of protons are diffused by the EGMF. We also find event clusterings in the direction of nearby sources or source clusterings. Such event clusterings will not be hidden by a structured EGMF, although their angular scale will be spread. At 500 event detections, the event clusterings will increase, and the local structure of the universe will appear.

A larger cell size used to calculate the correlation coefficients is expected to lead to larger correlation coefficients, since the EGMF obscures UHECR arrival directions, as mentioned above. Figure 4 shows the same example as Figure 2, but the size of the cell is chosen to be $4^\circ \times 4^\circ$. The correlation coefficients are larger than those in Figure 2 for all panels. The increase is clear even in the case of $B = 0.0 \mu\text{G}$, since some arriving cosmic rays from a source will be distributed on a small scale, but one larger than 2° , due to the finite angular resolution of UHECR experiments. The values of the coefficients do not increase even if the size of the cell is larger than $4^\circ \times 4^\circ$. In this figure, we find that the numbers of events required for the convergence of the correlation coefficients is almost unchanged.

5. DISCUSSION AND CONCLUSIONS

In this paper, we calculated the arrival distribution of UHE protons, taking into account energy losses and deflections by the EGMF during propagation in intergalactic space, in order to investigate the possibility that future observations of UHECRs may be able to unveil the local structure of UHE universe, even considering the strength and structure of the EGMF. In order to reproduce a realistic situation, we adopted a structured EGMF model and source distributions which reproduce the observed local structure. The arrival distribution of UHE protons was compared statistically to their source distribution using correlation coefficients. As the number of observed events increases, the correlation coefficient increases, and converges to some value which represents the ability to discern the source distribution via UHE protons, i.e., charged particles. Thus, the number of events at which the correlation coefficient starts to converge is an important number for UHECR observations, as the detection of this critical number of events will allow us to unravel the UHECR source distribution. We found that UHECRs above $10^{19.8}$ eV are the best indicators for deciphering their source distribution within 100 Mpc, from a discussion based on the final values of the correlation coefficients and the GZK mechanism; 5000, 500, and 200 event detections above $10^{19.8}$ eV on all the sky can reveal their source distribution for source number densities of 10^{-4} , 10^{-5} , and 10^{-6}Mpc^{-3} , respectively. Note that ground-based detectors observe only about half of the hemisphere, so only half this number are required.

We assumed that all UHECRs are protons. However, some fraction of heavier components is possible, as mentioned in § 1. Heavier components experienced larger deflections by EGMF, and thus the positional correlation becomes worse, which would increase the number of detected events required to unveil the local UHECR source distribution.

In this study, we only considered EGMF as the source of magnetic field, i.e., neglected the GMF, which also deflects trajectories of UHE protons efficiently by its regular spiral and dipole components (Alvarez-Muniz et al. 2002; Yoshiguchi et al. 2003b). A turbulent component of the GMF would very weakly change the arrival direction of UHE protons (Yoshiguchi et al. 2004). The deflection angles of UHECR protons are a few degrees even at around 10^{20} eV, except in the direction of Galactic center. This deflection might disturb the spatial pattern of the UHECR arrival distribution on the scale of a few degrees. The effect of the GMF will be the subject of future investigation.

Another approach to exploring UHECR sources has also been suggested by Cuoco et al. (2007). These authors suggested that a global comparison of the two-point correlation function of the data with one of the catalogs of potential source candidates would be a powerful diagnostic tool for source-class identification. They claim that this method is less sensitive to the deflection of UHECRs in magnetic fields, being an indirect observation of the sources. On the other hand, our method is a direct observation of the sources and source distribution, and is useful as long as the actual EGMF is not strong, as in our model, and heavy components do not dominate CRs at the highest energies.

We adopt 2.6 as a spectral index for UHECR emission in the sources to reproduce the observed spectra above 10^{19} eV (except for super-GZK events cataloged by AGASA). The observed spectra can also be reproduced within a model of the E^{-2} injection spectrum in the sources by varying E_{max} from source to source with a power-law distribution (Kachelriess & Semikoz 2006), although the power-law index of the distribution is fine-tuning. If the latter scenario is real, the number of detected events required to unveil sources that can contribute arriving cosmic rays above certain energy threshold may be smaller than that in our scenario, since there are many sources whose E_{max} is smaller than our energy thresholds of $10^{19.6}$, $10^{19.8}$, and 10^{20} eV. Such sources should be observed through lower energy cosmic rays. However, lower energy cosmic rays are more deflected by the EGMF, so it may be difficult by our method to know the positional distribution of such sources.

A number of studies of the UHECR source number density have found results of around 10^{-5}Mpc^{-3} based on the AGASA results, as discussed in § 1. If this number density is accurate, 5 years of observation by Auger and future observations by the TA and the Extreme Universe Space Observatory (Ebisuzaki et al. 2007) should be sufficient to reveal the distribution of nearby UHECR sources. The dawn of UHE particle astronomy is just around the corner.

The work of H.T. is supported by Grants-in-Aid for JSPS Fellows. The work of K.S. is supported by Grants-in-Aid for Scientific Research provided by the Ministry of Education, Science and Culture of Japan through research grant S19104006.

REFERENCES

- Abbasi, R. U., et al. 2005a, *ApJ*, 623, 164
 ———. 2005b, *ApJ*, 622, 910
 Aloisio, R., et al. 2007, *Astropart. Phys.*, 27, 76
 Alvarez-Muniz, J., Engel, R., & Stanev, T. 2002, *ApJ*, 572, 185
 Bagchi, J., et al. 2002, *NewA*, 7, 249
 Berezhinsky, V., & Grigorjeva, S. I. 1988, *A&A*, 199, 1
 Blasi, P., & de Marco, D. 2004, *Astropart. Phys.*, 20, 559
 Chodorowski, M. J., Zdziarske, A. A., & Sikora, M. 1992, *ApJ*, 400, 181
 Cuoco, A., et al. 2007, preprint (arXiv: 0709.2712)
 De Marco, D., Blasi, P., & Olinto, A. V. 2003, *Astropart. Phys.*, 20, 53
 Dolag, K., et al. 2005, *J. Cosmol. Astropart. Phys.*, 0501, 009
 Ebisuzaki et al. 2007, *Proc. 30th Int. Cosmic Ray Conf. (Merida)*, 831
 Engel, R., et al. 2007, preprint (arXiv:0706.1921)
 Fukushima et al. 2007, *Proc. 30th Int. Cosmic Ray Conf. (Merida)*, 955
 Giovannini, G., & Feretti, L. 2000, *NewA*, 5, 335
 Glushkov, A. V., et al. 2007, preprint (arXiv:0710.5508)
 Gorbunov, D. S., & Troitsky, S. V. 2005, *Astropart. Phys.*, 23, 175
 Greisen, K. 1966, *Phys. Rev. Lett.*, 16, 74

- Hague, J. D., et al. 2007, *Astropart. Phys.*, 27, 134
Hayashida, N., et al. 2000, *AJ*, 120, 2190
Kachelriess, M., & Semikoz, D. 2005, *Astropart. Phys.*, 23, 486
———. 2006, *Phys. Lett.*, B634, 143
Kim, K. T., et al. 1989, *Nature*, 341, 720
Kronberg, P. P. 1994, *Rep. Prog. Phys.*, 57, 325
Mollerach, S., et al. (Pierre Auger Collaboration), 2007, preprint (arXiv:0706.1749)
Mucke, A., et al. 2000, *Comput. Phys. Commun.*, 124, 290
Roth, M., et al. (Pierre Auger Collaboration). 2007, preprint (arXiv:0706.2096)
Saunders, W., et al. 2000, *MNRAS*, 317, 55
Sigl, G., Miniati, F., & Ensslin, T. A. 2003, *Phys. Rev. D*, 68, 043002
Takami, H., & Sato, K. 2008, *Astropart. Phys.*, 28, 529
Takami, H., Yoshiguchi, H., & Sato, K. 2006, *ApJ*, 639, 803 (erratum 653, 1584 [2006])
Takeda, M., et al. 1999, *ApJ*, 522, 225
Takeuchi, T. T., Yoshikawa, K., & Ishii, T. T. 2003, *ApJ*, 587, L89 (erratum 606, L171 [2004])
Tinyakov, P. G., & Tkachev, I. I. 2001, *J. Exp. Theor. Phys. Lett.*, 74, 445
———. 2002, *Astropart. Phys.*, 18, 165
Uchihori, Y., et al. 2000, *Astropart. Phys.*, 13, 151
Unger, M., et al. (Pierre Auger Collaboration). 2007, preprint (arXiv: 0706.1495)
Yoshiguchi, H., Nagataki, S., & Sato, K. 2003a, *ApJ*, 592, 311
———. 2003b, *ApJ*, 596, 1044
———. 2004, *ApJ*, 607, 840
Yoshida, S., & Teshima, M. 1993, *Prog. Theor. Phys.*, 89, 833
Zatsepin, G. T., & Kuz'min, V. A. 1966, *J. Exp. Theor. Phys. Lett.*, 4, 78